

# Methylglyoxal Inhibits the Binding Step of Collagen Phagocytosis\*

Received for publication, October 19, 2006, and in revised form, January 16, 2007. Published, JBC Papers in Press, January 17, 2007, DOI 10.1074/jbc.M609859200

Sandra A. C. Chong<sup>‡</sup>, Wilson Lee<sup>‡</sup>, Pam D. Arora<sup>‡</sup>, Carol Laschinger<sup>‡</sup>, Edmond W. K. Young<sup>§</sup>, Craig A. Simmons<sup>§</sup>, Morris Manolson<sup>‡</sup>, Jaro Sodek<sup>‡</sup>, and Christopher A. McCulloch<sup>†1</sup>

From the <sup>‡</sup>Canadian Institutes of Health Research Group in Matrix Dynamics, University of Toronto, Toronto, Ontario M5S 3E2, Canada and the <sup>§</sup>Department of Mechanical and Industrial Engineering, University of Toronto, Toronto, Ontario M5S 3E2, Canada

Bacterial infection-induced fibrosis affects a wide variety of tissues, including the periodontium, but the mechanisms that dysregulate matrix turnover and mediate fibrosis are not defined. Since collagen turnover by phagocytosis is an important pathway for matrix remodeling, we studied the effect of the bacterial and eukaryotic cell metabolite, methylglyoxal (MGO), on the binding step of phagocytosis by periodontal fibroblasts. Type 1 collagen was treated with various concentrations of methylglyoxal, an important glucose metabolite that modifies Arg and Lys residues. The extent of MGO-induced modifications was authenticated by amino acid analysis, solubility, and cross-linking. Cells were incubated with fluorescent beads coated with collagen, and the percentage of phagocytic cells was estimated by flow cytometry. MGO inhibited collagen binding (20% of control for 10 mM MGO) in a time- and concentration-dependent manner. MGO-induced inhibition of binding was prevented by aminoguanidine, which blocks the formation of collagen cross-links. MGO reduced collagen binding strength and blocked intracellular calcium signaling. MGO modified the Arg residue in the critical  $\alpha_2\beta_1$  integrin-binding recognition sequence of triple helical collagen peptides, whereas MGO-induced cross-linking of Lys residues played only a small role in binding inhibition. Thus, MGO modifications of Arg residues in collagen could be a key factor in the impaired degradation of collagen that promotes fibrosis in chronic infections, such as periodontitis.

Connective tissue homeostasis is maintained by fibroblasts that can synthesize and degrade the collagenous matrix in response to changes in physiological and pathological conditions. Disruptions to the balance of matrix remodeling may lead to net loss of collagen or to disorganized overgrowth of collagen in several pathological conditions (1). In chronic infections of connective tissues, such as periodontitis, bacterial cell metabolites (2) disrupt matrix homeostasis and promote collagen loss and fibrosis in collagen-rich tissues (1). At least part of this loss of homeostasis has been attributed to infection-induced

increase of collagen synthesis and impaired collagen degradation (3, 4). Although an intracellular phagocytic pathway of collagen degradation by fibroblasts is known to be important for maintaining homeostasis in mature connective tissues (5), the effect of bacterial and eukaryotic cell metabolites on collagen phagocytosis has not been defined.

The recognition and binding of collagen molecules by cell surface receptors is the initial, rate-limiting step in collagen phagocytosis by fibroblasts. The principal receptor for type I fibrillar collagen is the  $\alpha_2\beta_1$  integrin (6–10), which is a critical mediator of the binding step of collagen phagocytosis (11, 12). Integrins are composed of transmembrane  $\alpha$  and  $\beta$  subunits. Each subunit exhibits a large extracellular domain, a single-pass transmembrane domain, and a small cytoplasmic tail. The N terminus of the integrin  $\alpha_2$ -subunit encompasses a 7-fold repeat. Between repeats II and III, as well as in several other  $\alpha$ -subunits, are an additional 200 amino acids designated as the A (or I) domain (13). The A domain can regulate cell binding to collagen by recognizing the Gly-Phe-hydroxyproline (Hyp)<sup>2</sup>-Gly-Glu-Arg motif in collagen, which is considered the principal collagen binding site for the  $\alpha_2\beta_1$  integrin (14–16).

Prolonged exposure of collagen to bacterial and eukaryotic cell glucose metabolites affects collagen structure by forming intermolecular cross-links that can reduce the flexibility of connective tissues and reduce matrix turnover (17). Notably, MGO has been detected in the fluid draining from periodontitis infections (18), but the effect of MGO-induced modifications on the binding and internalization steps of collagen phagocytosis (which rely on the  $\alpha_2\beta_1$  integrin) has not been investigated. To define a potential role for phagocytosis in periodontitis-induced pathologies of connective tissues, we assessed the effect of MGO treatment of collagen on the  $\alpha_2\beta_1$  integrin-dependent binding step of collagen phagocytosis. Since collagen turnover in periodontal connective tissues is faster than in any other human tissue yet studied (19) and since cultured periodontal fibroblasts primarily express the  $\alpha_2\beta_1$  integrin (20), we used cells from the periodontium as a model system for defining the critical, rate-limiting steps in collagen phagocytosis. Here we provide evidence that MGO-induced modifications of the Gly-Phe-Hyp-Gly-Glu-Arg motif in collagen inhibit the collagen binding step of phagocytosis. These data suggest a mechanism that

\* This work was supported by the Canadian Institutes of Health Research and Alpha Omega. The costs of publication of this article were defrayed in part by the payment of page charges. This article must therefore be hereby marked "advertisement" in accordance with 18 U.S.C. Section 1734 solely to indicate this fact.

<sup>1</sup> To whom correspondence should be addressed. Rm. 244, Fitzgerald Bldg., 150 College St., Toronto, Ontario M5S 3E2, Canada. Tel.: 416-978-1258; Fax: 416-978-5956; E-mail: christopher.mcculloch@utoronto.ca.

<sup>2</sup> The abbreviations used are: Hyp, hydroxyproline; MGO, methylglyoxal; TRITC, tetramethylrhodamine isothiocyanate; PBS, Mg<sup>2+</sup>-, Ca<sup>2+</sup>-free phosphate-buffered saline; DAPI, 4',6-diamidino-2-phenylindole; APG, *p*-azido-phenyl glyoxal monohydrate; BSA, bovine serum albumin; PIPES, 1,4-piperazinediethanesulfonic acid.

explains how chronic bacterial infection in close proximity to connective tissues dysregulates collagen degradation, thereby leading to loss of connective tissue homeostasis.

## EXPERIMENTAL PROCEDURES

**Reagents**—Latex (2- $\mu\text{m}$  diameter) beads were purchased from Polysciences (Warrington, PA). Antibodies to  $\beta$ -actin (clone AC-15), TRITC-phalloidin, 4',6-diamidino-2-phenylindole (DAPI), D-ribose, MGO (Sigma catalogue number M0252), aminoguanidine, and maleic anhydride were from Sigma. Bovine serum albumin was purchased from Calbiochem. Carboxyl ferromagnetic beads (2–2.9  $\mu\text{m}$ ) were purchased from Spherotech (Libertyville, IL). Triple helical collagen peptides (36 amino acids) mimicking the  $\alpha_2\beta_1$  integrin binding site of collagen were obtained from Dr. G. Fields (Florida Atlantic University, Boca Raton, FL). Bacterial collagenase was from Worthington. Activating  $\alpha_2$  integrin antibody (JBS2) and antibody to  $\alpha_2$  integrin (AB1936) were purchased from Chemicon International (Temecula, CA). Activating  $\beta_1$  integrin antibody (CD29 mouse anti-human) was obtained from Serotec (Raleigh, NC). Antibody to the discoidin domain receptor 1 (c-20/sc-532) was from Santa Cruz Biotechnology, Inc. (Santa Cruz, CA). Antibody to  $\beta_1$  integrin (4B4) was from Beckman-Coulter (Burlington, Ontario, Canada). Antibody to  $\alpha_2$  integrin (P1E6) was from Chemicon. Antibody to methylglyoxal-AGE (Arg-pyrimidine) was from Biologo (Germany). The protein cross-linker *p*-azidophenyl glyoxal monohydrate (APG) was obtained from Pierce.

**Cell Culture and Human Gingival Tissues**—Human gingival fibroblasts (passages 4–10) were derived from primary explant cultures as described previously (21). Cells were grown in  $\alpha$ -minimal essential medium, 15% (v/v) fetal bovine serum, and 10% antibiotics, maintained at 37 °C in a humidified incubator containing 5% CO<sub>2</sub>, and were passaged with 0.01% trypsin. Rat-2 fibroblasts (ATCC CRL 1764; American Type Culture Collection) were subcultured from frozen stocks and incubated in Dulbecco's modified Eagle's medium (high glucose) containing 10% fetal bovine serum and antibiotics. Discoidin domain receptor 1<sup>+/+</sup> (DDR1<sup>+/+</sup>) and DDR1<sup>-/-</sup> fibroblasts (kindly donated by W. Vogel (University of Toronto) were passaged with 0.25% trypsin plus 1 mM EDTA and grown in similar medium as above. For examination of MGO-induced alterations of tissues *in situ*, biopsies of human gingiva from healthy and periodontitis-affected human subjects were obtained (*n* = 3 subjects each) and fixed with paraformaldehyde, and histological sections were prepared for immunostaining. The biopsies were obtained with informed consent according to the specifications of the Health Sciences Research Ethics Board at the University of Toronto.

**Collagen Beads**—Collagen-coated latex beads were prepared as previously described (20). Briefly, beads were incubated with 1 ml of an acidic solution of bovine type I collagen (2.9 mg/ml; Vitrogen, Cohesion Technologies), neutralized with 100  $\mu\text{l}$  of 1 N NaOH to pH 7.4 to facilitate fibril formation on the beads, vortexed, and incubated at 37 °C for 10 min. This time period is known to allow stable fibril formation on the beads (22). BSA-coated beads were prepared by incubating latex beads with 1 ml of 1% (w/v) BSA for 30 min at 37 °C. The beads were pelleted,

incubated with control or MGO-containing medium (see below), sonicated in solution for 10 s, and incubated overnight at 37 °C in a humidified incubator containing 5% CO<sub>2</sub>.

Collagen was treated with 0.1, 1, or 10 mM MGO diluted in PBS overnight or up to 5 days at 37 °C. In some experiments, collagen was glycosylated with 0.5 M D-ribose for up to 5 days at 37 °C. Control collagen was prepared in parallel in Mg<sup>2+</sup>-, Ca<sup>2+</sup>-free phosphate-buffered saline (PBS) for both methods. After incubation, the beads were pelleted, washed with PBS, resuspended in PBS, and counted prior to incubation with cells. Evaluation of equal loading of collagen on beads was done by immunoblotting of bead-associated collagen as described (23). For assessment of bead-associated proteins, identical procedures were used, except proteins were coated on magnetite beads. Inhibition of MGO-induced cross-linking was obtained by aminoguanidine (20 mM) co-incubation of collagen-coated beads overnight.

**Analysis of Cross-linked Collagen**—The relative abundance of cross-linking after MGO was estimated by analysis of hydroxyproline content after solubilization of collagen by pepsin digestion (50  $\mu\text{g}$  of pepsin/ml in 0.5 N acetic acid, 23 °C, 16 h) followed by amino acid analysis using high pressure liquid chromatography (Alliance 1690; Waters; Milford, MA; Hospital for Sick Children, Toronto, Canada). For SDS-PAGE, sample buffer (50  $\mu\text{l}$ ; 62.5 mM Tris-HCl, pH 6.8, 2% SDS, 10% glycerol, 50 mM dithiothreitol) was added to control, collagen-coated beads or MGO-treated beads. Samples were prepared by heating beads to 50 °C for 30 min, and the eluates were analyzed by SDS-PAGE (7.5% acrylamide) followed by silver staining.

**Adhesion Assays and Flow Cytometry**—Cells were counted electronically, and collagen beads (yellow-green fluorescent beads; Ex<sub>max</sub> = 485 nm, Em<sub>max</sub> = 515 nm) were loaded on to the top (*i.e.* dorsal) surfaces of cells at a 6:1 bead/cell ratio. After incubation of beads with cells for defined time periods, cells were washed (PBS), detached with 0.01% trypsin from culture dishes, and resuspended in PBS, a process that removes loosely attached, nonspecifically bound beads (24, 25). Samples of cells were analyzed for bead binding by flow cytometry (Beckman-Coulter Altra, Miami, FL) to estimate the percentage of cells with bound fluorescent beads and the relative number of beads per cell. For  $\beta_1$  or  $\alpha_2$  integrin-blocking experiments, cells were preincubated with 4B4 antibody (1  $\mu\text{g}/\text{ml}$ ) or P1E6 (2  $\mu\text{g}/\text{ml}$ ), respectively, incubated with beads for 1 h, washed with PBS, trypsinized, and analyzed by flow cytometry. Similarly, for  $\alpha_2$  and  $\beta_1$  integrin activation, JBS2 mouse anti-human monoclonal antibody (10  $\mu\text{g}/\text{ml}$ ) or CD29 mouse anti-human (10  $\mu\text{g}/\text{ml}$ ) was added prior to collagen-coated bead exposure and flow cytometry analysis as described (4).

Evaluation of collagen bead internalization was conducted as previously described (11). Briefly, fluorescein isothiocyanate/collagen-coated beads were incubated for specific times with cells, and subsequent internalization was blocked by cooling on ice. Fluorescence from extracellular beads was quenched by trypan blue, thereby permitting fluorescence microscopic discrimination and quantification of external (quenched) and internalized (nonquenched) beads.

**Binding Strength Assay**—The relative binding strength of collagen beads to cells was estimated by a shear wash assay (4, 26)

## MGO Inhibits the Binding Step of Collagen Phagocytosis

in which binding of beads to cells was examined *in situ*. Cells grown in monolayer culture (24-well plates) were incubated with control or glycated collagen-coated fluorescence beads for 1 h and subjected to increasing numbers of washes with PBS from 1 to 32 washes with a repeating pipettor (Eppendorf). Cells were fixed with 3.7% formaldehyde for 15 min, permeabilized with Triton X-100, washed with PBS, stained with DAPI (5  $\mu\text{g}/\text{ml}$ ), and air-dried. DAPI-stained nuclei were used to identify the location of each cell, and the number of bound beads associated with each cell was counted by fluorescence microscopy in a 5-mm wide circular zone in the middle of the well. For each experiment, at least 50 cells were counted in each well, and four wells were evaluated for each experiment. The experiment was repeated three times. During washing with the pipette, cells adhered to the bottom of the culture dish experience local shear stress due to radial outflow of the ejected fluid over the cell layer. The shear stress on the cells can be approximated for wall shear stress produced by the normal impingement of an axisymmetric jet on a planar surface. According to Phares *et al.* (27), the wall shear stress varies radially outward from the stagnation point (the point at which the jet initially hits the cell surface), increasing to a maximum value ( $\tau_{\text{max}}$ ) governed by the following.

$$\tau_{\text{max}} = 44.6\rho u_0^2 \text{Re}_0^{-1/2} \left(\frac{H}{D}\right)^{-2} \quad (\text{Eq. 1})$$

In this equation,  $\rho$  represents the fluid density,  $H$  is the jet height from the planar surface,  $D$  is the nozzle diameter,  $u_0$  is the jet exit velocity, and  $\text{Re}_0 = u_0 D/\nu$  is the jet Reynolds number, where  $\nu$  is the fluid kinematic viscosity. This maximum shear stress occurs at a radial distance of  $r_{\text{max}} = 0.09H$  from the jet axis (27). In these experiments, the pipette tip diameter was  $D \sim 0.8$  mm, the volumetric flow rate was  $Q \sim 250$   $\mu\text{l}/\text{s}$ , jet height was estimated to be  $H \sim 10$  mm, and fluid properties were approximately those of water. Thus,  $u_0 \sim 0.5$  m/s and  $\text{Re}_0 \sim 400$ , resulting in a maximum shear stress of  $\tau_{\text{max}} \sim 3.5$  pascals (or 35 dynes/cm<sup>2</sup>) at  $r_{\text{max}} \sim 0.9$  mm.

**Cell Spreading**—Type I fibrillar collagen-coated plates (Bio-coat Cell Environments; BD Biosciences) were treated overnight with MGO or with control vehicle. Cells were plated and spread for 1, 2, and 4 h, washed with PBS, fixed with 3.7% formaldehyde, permeabilized with 0.2% Triton X-100, and stained with rhodamine-phalloidin (5  $\mu\text{M}$ ). Cells were washed and air-dried, and coverslips were mounted with anti-fade solution. Cells were photographed, and projected surface areas were measured by digital morphometry.

**[Ca<sup>2+</sup>]<sub>i</sub> Measurements**—Nonfluorescent latex beads were coated with collagen and glycated overnight with MGO. Beads were applied to cells that were loaded with fura 2/acetoxymethyl ester (3  $\mu\text{M}$ ). Intracellular calcium concentration ([Ca<sup>2+</sup>]<sub>i</sub>) was measured with a microscope-based, ratio fluorimeter over time (28). Only cells that exhibited bound collagen-coated beads were measured.

**Immunoblotting**—Cells were spread over type I collagen or MGO-treated collagen-coated plates for specific time periods. After spreading, cells were washed with PBS and extracted with SDS-sample buffer. Protein concentrations were measured

with the Bio-Rad assay using BSA as a standard. The relative amounts of proteins were normalized for all samples. Proteins were separated on 7.5–10% gradient SDS-polyacrylamide gels under nonreducing conditions and transferred to nitrocellulose. Blots were probed with appropriate antibodies for  $\alpha_2$  integrin or DDR1. Immunoblots were developed by chemiluminescence (ECL; Amersham Biosciences).

Bead-associated proteins including integrins and DDR1 were analyzed as previously described (29). Briefly, control and MGO-treated collagen-coated magnetite beads were added to cells for 1 h. After incubation, medium was removed, and the cells were washed to remove loosely bound beads. Cells and beads were scraped with cytoskeletal extraction buffer (0.5% Triton X-100, 50 mM NaCl, 300 mM phenylmethylsulfonyl fluoride, 10 mM PIPES, and 1  $\mu\text{M}$  phalloidin, pH 6.8). Magnetite beads were isolated with a magnet (Dyna) at 4 °C, washed with cytoskeletal extraction buffer, and pelleted, and bead-associated proteins were released during 20-s sonication in SDS-sample buffer. Beads were removed and counted to estimate relative protein concentrations in samples. Differences in the relative amounts of total proteins were normalized between samples, and proteins were analyzed by immunoblotting as described above.

**Cross-linking of Collagen**—Collagen-coated beads were incubated overnight at 37 °C with APG (10 mM; pH 7). Beads were incubated on ice, and cross-linking was activated by UV light (8 min; 2  $\times$  15 watts at a distance of 5 cm) and verified by SDS-PAGE. The beads were pelleted and washed. Incubation of collagen beads with cells was performed as described above prior to flow cytometry analysis.

**Inhibition of MGO-induced Lysine Cross-linking of Collagen**—Collagen-coated beads were treated with maleic anhydride to protect lysine sites from MGO-induced cross-linking. Collagen-coated beads were incubated overnight with MGO (10 mM; 37 °C). In some experiments, maleic anhydride protection was reversed by incubating beads at pH 9 prior to MGO treatment. Collagen bead binding methods were used as described above, followed by analysis with flow cytometry. Collagen beads treated with maleic anhydride alone served as controls.

**Mass Spectrometry**—Triple helical collagen peptides encompassing the  $\alpha_2\beta_1$  integrin binding site of collagen (0.5 mg of peptide at 50 nM) were dissolved in PBS and treated overnight at 37 °C with 10 mM MGO. Excess reagent was removed using protein-desalting spin columns (Pierce) and equilibrated in 25 mM ammonium bicarbonate. MGO-treated peptide (25 nM) was vacuum-dried prior to mass spectrometry (Hospital for Sick Children). The remaining 25 nM peptide was digested with trypsin (in 25 mM NH<sub>4</sub>HCO<sub>3</sub>) to give an E/S ratio of 1:500. The digestion was allowed to proceed overnight at 37 °C, evaporated to dryness, and analyzed on a Micromass electrospray ionization quantitative time-of-flight mass spectrometer coupled with a Waters CapLC high pressure liquid chromatography system (Hospital for Sick Children).

**Statistical Analyses**—For all data sets, experiments were repeated at least three times, and each repeat contained three replicates. For quantitative data, means and S.E. were calculated. Comparisons between samples were performed using either Student's *t* test or single factor analysis of variance fol-

lowed by Scheffe's test for individual differences. Statistical significance was set at  $p < 0.05$ .

## RESULTS

**Collagen Model System**—We incubated collagen with MGO (30) for 19 h or with D-ribose for time periods up to 5 days (31, 32). Treatment of collagen with D-ribose (5 days of treatment) inhibited collagen binding to cells ( $38.0 \pm 3.5\%$  of controls;  $n = 4$ ;  $p < 0.01$ ), but overnight treatments with MGO were more inhibitory ( $23.6 \pm 11.1\%$  of controls for 1 mM MGO;  $14.4 \pm 1.7\%$  of controls for 10 mM MGO;  $n = 4$ ;  $p < 0.001$ ). All further experiments were performed with MGO-treated collagen, since the treatments were more efficacious and required less time.

**MGO-treated Collagen**—The efficacy of the MGO treatment of collagen bound to beads was examined by amino acid analysis of eluted collagen from beads. With increasing concentrations of MGO, there were reduced ratios of Arg to hydroxyproline (Table 1). Since MGO treatment of Arg forms imidazolones that hydrolyze to ornithine (33), we also

**TABLE 1**  
MGO-induced modification of collagen

Latex beads were coated with collagen and then treated with MGO at the indicated concentrations as described under "Experimental Procedures." Collagen was eluted from beads and subjected to amino acid analysis. The relative amounts of Arg, hydroxyproline (OH-Pro), and ornithine were quantified from three independent samples. MGO treatment of Arg residues forms imidazolones, which hydrolyze to ornithine.

[MGO]	Arg/OH-Pro ratio	Ornithine/OH-Pro ratio
mM		
0	$0.56 \pm 0.07$	$0.003 \pm 0.001$
1	$0.30 \pm 0.04$	$0.015 \pm 0.004$
10	$0.09 \pm 0.03$	$0.031 \pm 0.009$

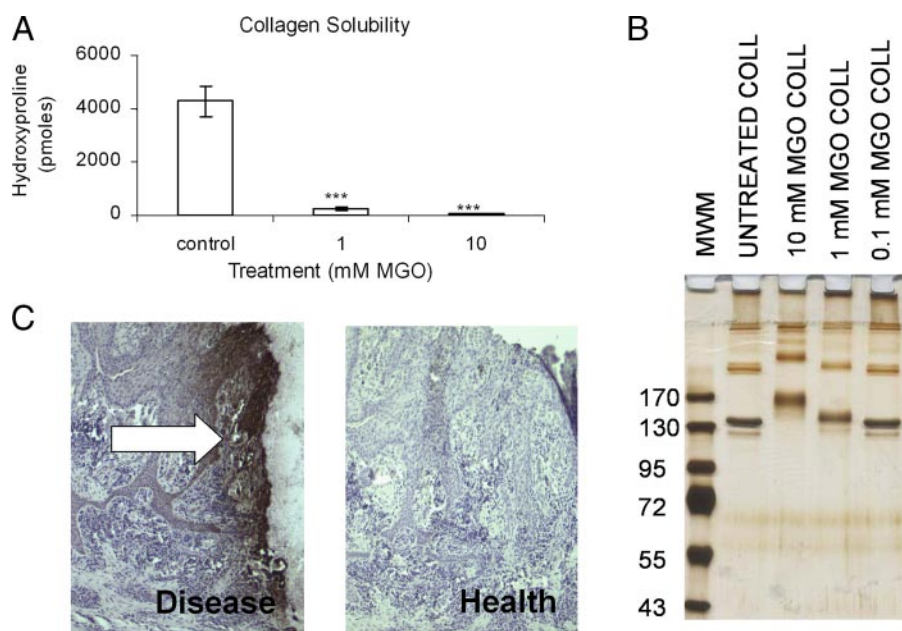


**FIGURE 1. Validation of MGO treatment of collagen.** *A*, collagen solubility after MGO treatment assessed by hydroxyproline content. Data are mean  $\pm$  S.E. of hydroxyproline content. \*\*\*,  $p < 0.001$  versus control (PBS). *B*, SDS-PAGE analysis of collagen gels after MGO treatment (10 mM). MGO, particularly at 10 mM, promotes cross-linking of collagen monomers into larger aggregates. *C*, healthy and periodontitis-affected human gingival connective tissues immunostained for MGO. The arrow points to lateral surface of periodontitis pocket wall that is stained heavily for MGO.

measured ornithine/hydroxyproline ratios, which increased with higher concentrations of MGO. The solubility of MGO-treated collagen samples was tested by pepsin digestion, followed by measurement of hydroxyproline content in the soluble fraction. Complete solubilization of control collagen was obtained after 16-h pepsin treatment, whereas MGO-treated collagen (1 and 10 mM) showed limited solubilization, even after 24 h of pepsin digestion. Of the material that was solubilized in pepsin-digested fractions, there was much less hydroxyproline content after treatment with higher concentrations of MGO (Fig. 1A). From SDS-PAGE analysis, we also found evidence for higher molecular mass aggregates of collagen molecules after MGO treatment, which is suggestive of increased collagen cross-linking (Fig. 1B) or possibly altered charge profile due to MGO derivatization.

We examined human gingival tissue samples removed from either healthy ( $n = 3$ ) or periodontitis-affected lesions ( $n = 3$ ) and, following paraformaldehyde fixation, immunostained these samples for MGO adducts with a monoclonal antibody to methylglyoxal-AGE (Arg-pyrimidine). These samples showed strong staining of the connective tissues adjacent to infected periodontal pockets but not in healthy tissues (Fig. 1C).

**Binding Step of Phagocytosis**—MGO treatment of collagen reduced collagen bead binding to cells to less than one-third of control values (Fig. 2A), and this effect was more pronounced at higher MGO doses (Fig. 2B;  $p < 0.01$ ). These effects were not attributable to a loss of collagen from beads, since measurements of bead-bound collagen by dot blotting (23) showed equivalent amounts of bound collagen, independent of MGO treatment (0.026 pg of collagen/bead after incubation in 3  $\mu$ M collagen solutions; 0.024 pg of collagen/bead after incubation in 3  $\mu$ M collagen solutions followed by MGO treatment). Cells were also incubated with BSA-coated beads to assess the specificity of the MGO treatment effect. There were low percentages ( $\sim 10\%$ ) of cells that bound BSA-coated beads (Fig. 2A); however, MGO treatments of BSA-coated beads exerted no effect on the percentages of cells with bound BSA beads. Reduced collagen bead binding was also observed in Rat-2 fibroblasts at equivalent reductions as human gingival fibroblasts (Fig. 2B).

We estimated collagen adhesion strength by comparing the relative proportion of cells that bound multiple beads when cells were incubated with beads at fixed bead/cell ratios. As reported earlier (11), cells exhibited a range of collagen bead binding in that most cells bound one bead, but a small population could bind four or more beads, presumably reflecting intrinsic heterogeneity in the affinity of collagen receptors in the cell population. Notably,

## MGO Inhibits the Binding Step of Collagen Phagocytosis

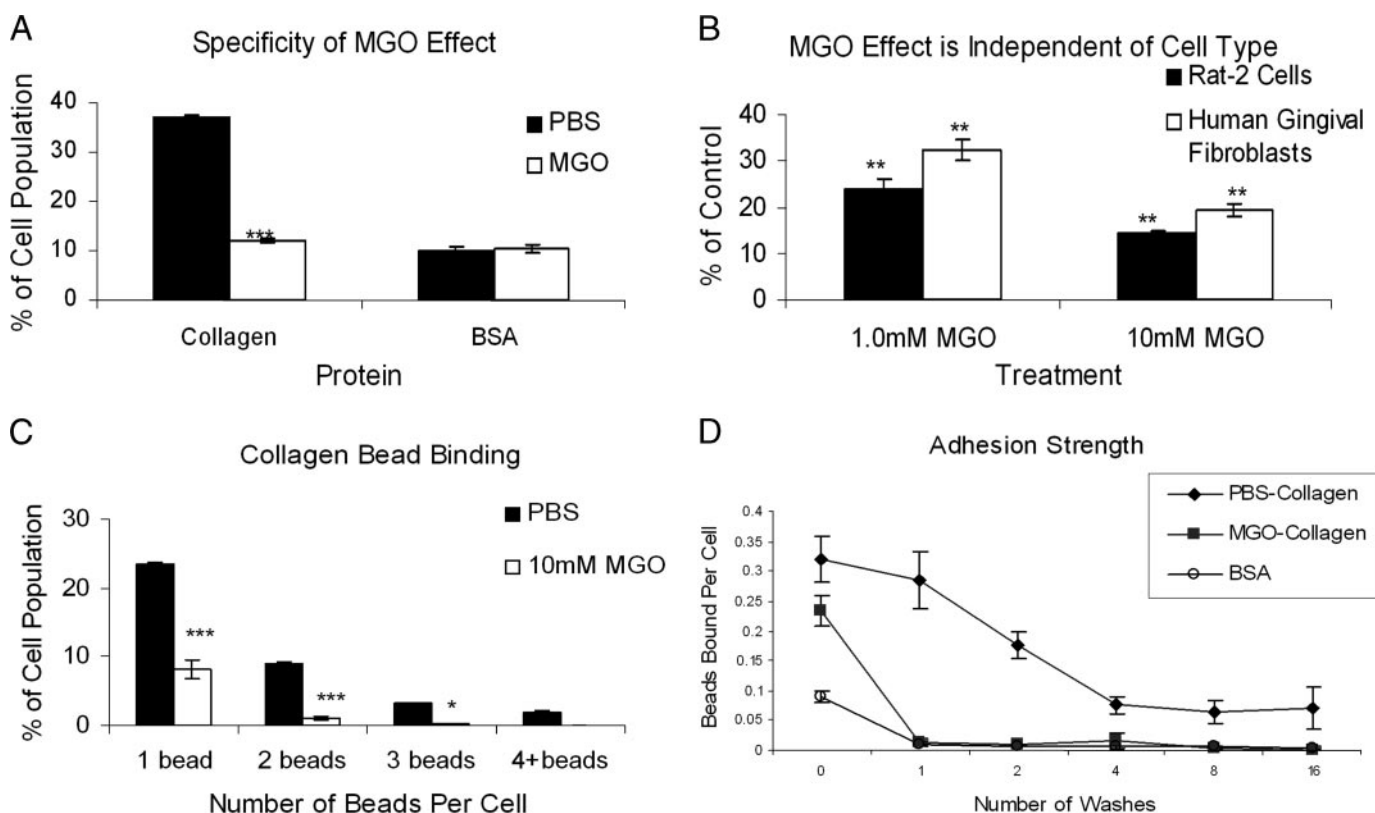


**FIGURE 2. Effect of MGO on cell binding to collagen.** Collagen-coated bead binding (6 beads/cell; 1-h incubation for all experiments; 3 independent samples/group). Data are mean  $\pm$  S.E. *A*, cells were incubated with collagen (control or 1 mM MGO-treated) or BSA-coated fluorescent beads (control or MGO-treated). For collagen beads, 1 mM MGO treatment reduced binding 3-fold compared with PBS control (\*\*\*,  $p < 0.001$ ). Binding of BSA-coated beads was unaffected by MGO treatment. *B*, Rat-2 cells and human gingival fibroblasts were incubated with PBS (control)- or MGO-treated collagen-coated beads. Data are percentages of cells binding MGO-collagen beads compared with PBS-treated collagen beads (\*\*\*,  $p < 0.001$  reduction compared with PBS control). *C*, cells were incubated with PBS (control) or MGO (10 mM) collagen-coated beads and assayed by flow cytometry for the percentage of cells binding 1, 2, 3, or 4 or more beads. \*\*\*,  $p < 0.0001$  MGO versus control; \*,  $p < 0.1$  MGO versus control. *D*, binding strength was estimated with a jet wash assay. The total number of beads bound to each DAPI-stained cell was counted and expressed as beads/cell. There were large reductions (less than one-tenth prior to washing) of binding for MGO-treated collagen and BSA beads after one wash ( $p < 0.001$ ) but only minimal reductions for collagen beads.

cultures of human gingival fibroblasts incubated with control collagen-coated beads showed higher percentages of cells with multiple bound beads compared with cultures exposed to MGO-treated collagen-coated beads, which usually exhibited binding of only one bead (Fig. 2C). These data indicated that MGO treatment may inhibit the binding strength of high affinity collagen receptors or that collagen beads may bind to each other under control conditions; conceivably, this interbead binding is inhibited by MGO. To examine these possibilities in more detail, we determined if beads adhered to each other under control and MGO conditions. At concentrations of beads that replicated the conditions used here but without cells, the distribution of bead interactions for untreated collagen beads was measured by flow cytometry: single beads, 94%; doublets, 5%; triplets, 0.3%; quadruplets, 0.06%. For 10 mM MGO-treated collagen beads, the distribution was as follows: single beads, 95%; doublets, 4%; triplets, 0.4%; quadruplets, 0.08%. We also examined the ability of the cells to bind collagen beads at high bead concentrations. We incubated beads with cells at bead/cell loading ratios of 4:1, 6:1, 8:1, 12:1, and 16:1. There was no observable plateau of bead binding when bead ratios were increased, even at bead/cell ratios of 16:1 (data not shown), indicating that under these experimental conditions, collagen receptors are not limiting.

**TABLE 2**  
Effect of MGO incubation times on collagen bead binding

Collagen beads were treated with vehicle or MGO (1 mM) for the indicated times and then incubated with Rat-2 cells for 1 h at 6 beads/cell. The percentage of cells with bound beads was estimated by flow cytometry. Data are mean  $\pm$  S.E. of the percentage of control cells for the indicated MGO treatment time. Between 16 and 122 h, there was no significant reduction of inhibition ( $p > 0.2$ ).

Duration of incubation	16 h	40 h	88 h	122 h
Collagen bead binding (percentage of controls)	52.3 $\pm$ 2.6%	68.1 $\pm$ 5.6%	63.9 $\pm$ 5.3%	46.6 $\pm$ 3.9%

With a more direct approach to measure the effect of MGO modifications on collagen binding, we estimated the strength of cell binding to collagen (4, 26). After an increasing number of jet washes, cells incubated with control beads showed progressively lower numbers of beads bound per cell, until reaching a plateau after four washes (Fig. 2D). In contrast, virtually all MGO-treated collagen beads were dislodged after one wash. BSA-coated beads were also washed off almost entirely after a single wash.

We determined whether the effect of MGO treatment on collagen binding could be increased by prolonged incubations of collagen with MGO. Only small differences of the percentage of cells binding collagen beads were evident between the different time periods (16–122 h; Table 2), indicating that the effect of MGO on collagen binding is maximized within 16 h. Inhibi-

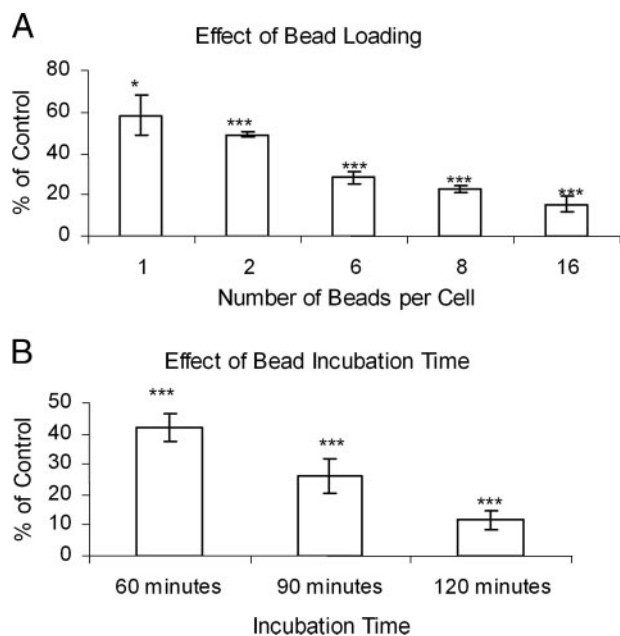


**FIGURE 3. MGO effect on collagen coated-bead binding.** Three independent samples were analyzed by flow cytometry for each group. Data are mean  $\pm$  S.E. of MGO-treated beads as a percentage of PBS control bead binding. *A*, cells were incubated with PBS control or 10 mM MGO collagen-coated beads at increasing bead/cell ratios. MGO effect was enhanced at higher bead/cell ratios. \*\*,  $p < 0.01$  versus PBS control; \*\*\*,  $p < 0.001$  versus control. *B*, cells were incubated with PBS (control) or 10 mM MGO collagen-coated beads for the indicated times and assayed for binding. The effect of MGO treatment was dependent on bead incubation time with cells. \*\*\*,  $p < 0.001$  MGO treatment versus PBS control.

tion of collagen binding was affected by collagen bead loading (Fig. 3A). Cells incubated with higher numbers of MGO-treated collagen-coated beads exhibited significantly reduced bead binding as a result of MGO treatment. The inhibition of collagen bead binding by MGO was also dependent on the duration of cell incubation times with beads, since there was greater inhibition of binding at longer time periods (Fig. 3B).

We assessed whether inhibition of collagen binding was a specific result of MGO-induced collagen cross-link formation. Aminoguanidine is a nucleophilic hydrazine compound that blocks the formation of glucose-derived collagen cross-links (34, 35). After overnight co-incubations of collagen beads with MGO and aminoguanidine, collagen bead binding was  $\sim 90\%$  of control levels ( $195 \pm 25.1\%$  for 1 mM MGO and  $323 \pm 14.0\%$  for 10 mM MGO; data are percentages of increases compared with MGO treatment alone).

**Cell Spreading and Intracellular Calcium**—Lamellipodial extension around fibrils is required for phagocytosis and intracellular digestion of collagen (12), a component process of phagocytosis that can be modeled by measuring cell spreading *in vitro* (11). After 1, 2, and 4 h of cell attachment to control or MGO-collagen, we quantified cell spreading by measuring projected cell surface area in cultures stained with rhodamine phalloidin (Fig. 4A). Cells were more rounded and exhibited  $<40\%$  of the surface area when plated on MGO-collagen compared with control collagen. The reduced spreading of cells on MGO-collagen was not due to cell death, since these cells spread normally when replated on control collagen.

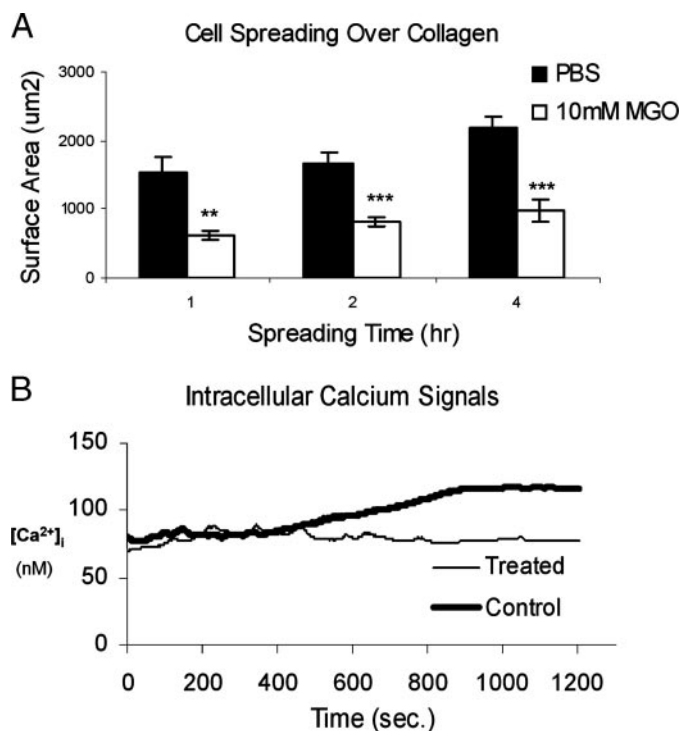


**FIGURE 4. MGO treatment of collagen inhibits cell spreading and calcium signaling.** *A*, cell spreading after 4 h on control or MGO-treated collagen gels. Actin filaments were stained with rhodamine phalloidin (500 $\times$ ). The projected surface area of cells was analyzed by morphometry after 1, 2, and 4 h. \*\*\*,  $p < 0.001$  MGO versus PBS control; \*\*,  $p < 0.01$  versus control. *B*, fura 2-loaded human gingival fibroblasts were incubated with PBS (control) collagen-coated beads or MGO (treated) collagen-coated beads. Intracellular calcium concentration ( $[Ca^{2+}]_i$ ) was estimated in single cells that bound collagen-coated beads. MGO collagen did not stimulate increased  $[Ca^{2+}]_i$  during lamellipodial extension. For both collagen and MGO-collagen beads, nine different cell samples were analyzed, and the mean increase of  $[Ca^{2+}]_i$  from one cell in each sample was computed.

During the initial phases of phagocytosis, when cells extend pseudopodia around collagen beads, intracellular free calcium ion concentration ( $[Ca^{2+}]_i$ ) is increased, or binding is strongly inhibited (36). Since matrix glycation can impair intracellular calcium signaling in endothelial cells (37), we measured  $[Ca^{2+}]_i$  following collagen bead binding to cells. In experiments using untreated control collagen beads (single cells in nine separate cultures), we found a slow, steady increase of  $[Ca^{2+}]_i$  with an increase of  $41 \pm 5$  nM  $Ca^{2+}$  over 20 min ( $p < 0.001$  compared with base line) (Fig. 4B), similar to a previous report (36). In contrast, cells that had bound MGO-treated collagen beads (single cells in nine separate cultures) showed no increase of  $[Ca^{2+}]_i$  after 20 min ( $p < 0.001$  collagen compared with MGO-collagen). This effect was not due to cell toxicity from the MGO bound to the collagen, since cells plated on MGO-treated tissue culture plastic exhibited increases of  $[Ca^{2+}]_i$  that were similar to controls (40 nM increase). As a second control, cells that were incubated with BSA-coated beads also showed no increase of  $[Ca^{2+}]_i$  (data not shown). Finally, to evaluate whether MGO-treated collagen quenched fura 2 fluorescence, we measured base line levels of  $[Ca^{2+}]_i$  but found no effect of the MGO on fura 2 fluorescence at the isosbestic point (356 nm excitation).

After binding to collagen, fibroblasts internalize the protein, which is then degraded in phagolysosomes (5). The effect of MGO on collagen internalization was estimated by incubating

# MGO Inhibits the Binding Step of Collagen Phagocytosis

**TABLE 3**

**Effect of MGO on collagen internalization**

Fluorescein isothiocyanate-collagen was attached to beads and treated with vehicle or MGO (10 mM; overnight or 16 h). Beads were incubated with Rat-2 cells (6 beads/cell) for 1, 2, or 4 h and examined by fluorescence microscopy. Fluorescence associated with external beads was quenched by trypan blue. The numbers of cells with internalized (fluorescent) beads were counted (top row, uncorrected). To determine whether the very low number of MGO-treated collagen beads that did bind to cells were indeed capable of being internalized, we adjusted for the greatly reduced numbers of cells binding MGO-treated collagen beads by counting only cells with bound beads (assessed by phase-contrast microscopy). At 10 mM MGO, this involved an ~4-fold correction. Data are expressed as the percentage of cells with internalized beads. For the uncorrected data (top row) there were significant reductions ( $p < 0.01$ ) at all time periods for the MGO effect. When corrections for binding were computed (bottom row), there was no significant effect of MGO treatment on collagen bead internalization for all time periods ( $p > 0.2$ ).

Time of incubation	1 h control	1 h MGO	2 h control	2 h MGO	4 h control	4 h MGO
Percentage of cells with internalized collagen beads (uncorrected for bead binding)	49 ± 7.9%	12 ± 3.6%	89 ± 8.8%	23 ± 4.4%	100 ± 0%	25 ± 6.6%
Percentage of cells with internalized collagen beads (corrected for bead binding)	52 ± 9.9%	68 ± 4.8%	85 ± 7.5%	92 ± 6.3%	100 ± 0%	100 ± 0%

cells with nonfluorescent beads coated with fluorescein isothiocyanate-collagen. Trypan blue quenching of collagen bead fluorescence was used to discriminate internalized from external beads. The number of internalized beads in 10 mM MGO-treated collagen was reduced to about one-quarter of control levels (Table 3). To determine whether the very low number of MGO-treated collagen beads that did bind to cells were indeed capable of being internalized, we adjusted for the greatly reduced binding of beads after MGO treatment and counted internalized beads in only those cells with bound beads. For cells that had bound one or more beads, there were no statistically significant differences ( $p > 0.2$ ) of internalized beads between control and MGO-treated samples (Table 3).

**Collagen Receptors**—Since MGO evidently affects the binding step of collagen phagocytosis but not the subsequent internalization step, we examined collagen bead-associated proteins to characterize the collagen receptors that may be affected by MGO. After a 1-h period of collagen bead binding, cells were lysed, and proteins associated with bound beads were immunoblotted to examine integrin  $\alpha_2$  subunit and DDR1, both of which are important receptors for fibrillar collagen (6, 38). When bead-associated proteins were examined, there was greatly reduced integrin  $\alpha_2$  subunit and DDR1 protein on MGO-collagen beads, an effect that was increased by higher concentrations of MGO (Fig. 5A). We also examined whether the lower numbers of MGO-collagen beads that bound to cells were indeed capable of interacting with these receptors. Accordingly, increased amounts of bead-associated proteins were loaded on gels to adjust for the lower numbers of bound beads. Under these experimental conditions, no increased integrin  $\alpha_2$  subunit was detected, but there was detectable signal for the DDR1 associated with 1 mM MGO and 10 mM MGO-treated collagen beads (Fig. 5A). These data indicated that the integrin  $\alpha_2$  subunit but not DDR1 is involved in MGO-reduced binding of collagen to cells.

We determined the functional contribution of the  $\alpha_2\beta_1$  integrin in collagen binding by preincubating cells with either an integrin  $\alpha_2$  subunit (P1E6) or integrin  $\beta_1$  subunit-inhibitory antibody (4B4) prior to exposure with collagen beads. After the addition of 4B4 antibody, binding of collagen beads was reduced to less than one-fifth of control values (Fig. 5B), in agreement with earlier data (20), indicating the importance of the integrin  $\beta_1$  subunit in fibrillar collagen binding by these cells. Similarly, treatment of cells with P1E6 antibody also reduced collagen bead binding to cells (one-fifth of control levels). As shown above, 10 mM MGO treatment of collagen reduced bead binding to one-quarter of control values. Incuba-

tion of MGO-treated collagen beads with the P1E6 antibody did not further reduce collagen binding. However, MGO treatment of collagen beads followed by incubation with the 4B4 antibody reduced binding further (Fig. 5B), indicating that in concert with the integrin  $\beta_1$  subunit, other integrin  $\alpha$  subunits are involved; this is consistent with previous findings of measurable but limited involvement of the  $\alpha_1\beta_1$  and  $\alpha_3\beta_1$  integrins in phagocytosis by human gingival fibroblasts (20).

Since bead binding could also be mediated by other, nonintegrin collagen receptors, we studied the effect of DDR1 in MGO-induced inhibition of collagen binding. Binding inhibition levels of DDR1<sup>-/-</sup> cells were compared with background-matched, DDR1<sup>+/+</sup> control cells. After 1 h of bead binding, analysis by flow cytometry showed only a minimal difference of MGO-mediated inhibition in DDR1 control and null cells (DDR1<sup>+/+</sup>-MGO-treated, 30.0 ± 2.9% of control collagen beads; DDR1<sup>-/-</sup>-MGO-treated, 26.6 ± 2.8% of control collagen beads;  $n = 3$  replicates/group;  $p > 0.2$ ). Thus, DDR1 had no measurable effect on the inhibitory effect of MGO on collagen bead binding.

We next studied whether the binding inhibition mediated by MGO could be reversed with activating antibodies to the integrin  $\alpha_2$  and  $\beta_1$  subunits. Human gingival fibroblasts were incubated with activating antibodies (for the integrin  $\alpha_2$  subunit JBS2 and for the integrin  $\beta_1$  subunit CD29) as described (4) prior to exposure to MGO-treated collagen beads. Although this treatment enhanced binding of untreated collagen beads, there was no enhancement of MGO-modified collagen binding after activation of the integrin  $\alpha_2$  and  $\beta_1$  subunits (1 collagen bead/cell; collagen binding of PBS control, 4.9 ± 0.7% of cell population; JBS2, 5.2 ± 0.9% of cell population; CD29, 4.4 ± 0.1% of cell population; JBS2 and CD29, 5.2 ± 0.8% of cell population), indicating that the MGO effect could not be reversed by antibody-induced collagen receptor activation. This effect was investigated further by analyzing human fibroblasts that were incubated with collagen or MGO-treated collagen beads and then immunostained with 12G10 antibody. This antibody recognizes an epitope in  $\beta_1$  integrins that is exposed on ligand binding (39). In cells incubated with collagen beads and then immunostained, there was prominent 12G10 staining around the collagen beads that was not present in cells incubated with MGO-collagen beads (Fig. 5C).

**Mechanism of Binding Inhibition**—Since MGO evidently increased cross-linking of collagen molecules (Fig. 1B), possibly by virtue of its capacity to modify Arg and Lys residues (30), we first explored the effect of collagen cross-linking by exposing

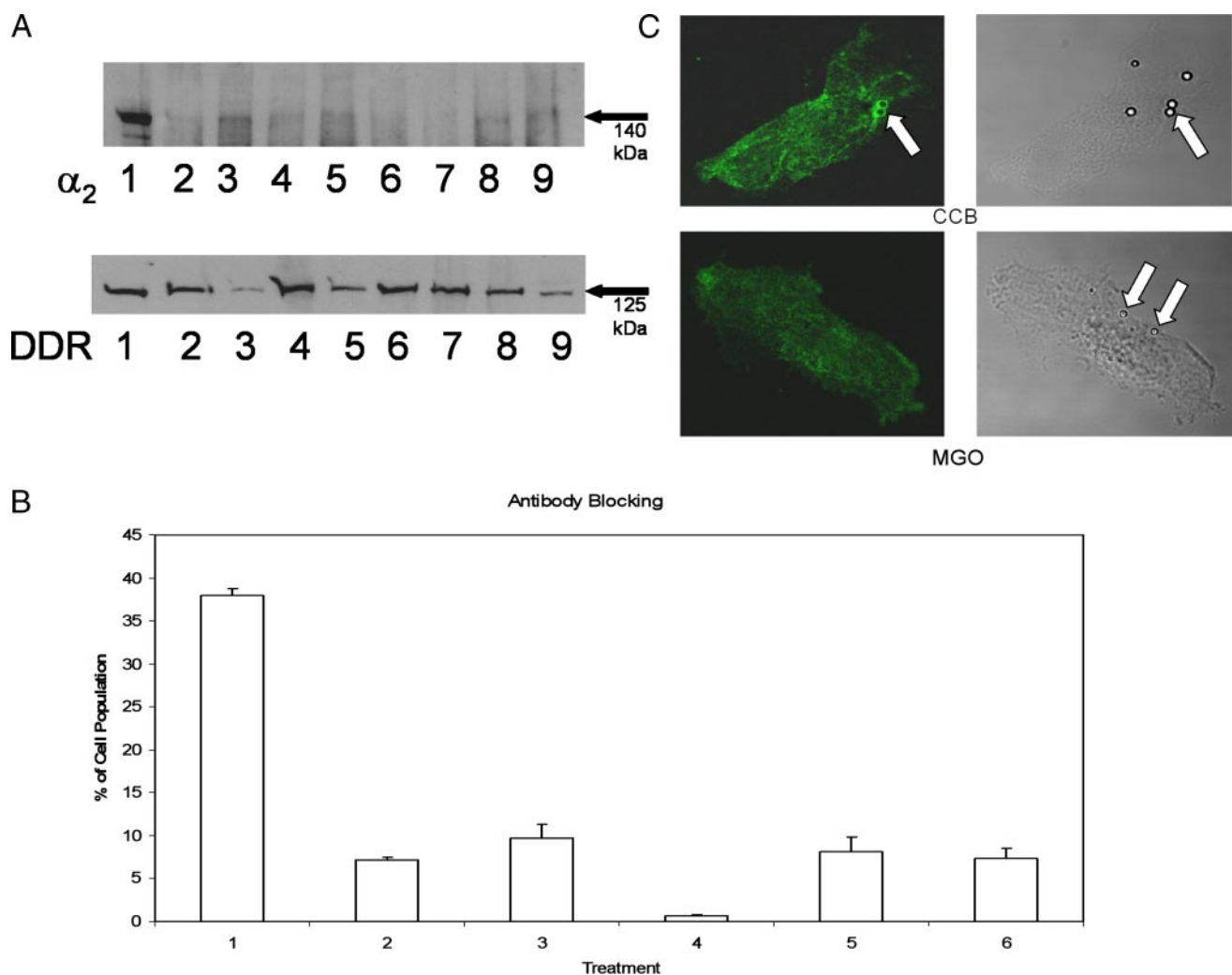


**FIGURE 5. MGO effects on collagen receptors.** *A*, cells were incubated with PBS or MGO (1 or 10 mM) collagen-coated magnetite beads. Cells were lysed, and bead-associated proteins were isolated and immunoblotted for integrin  $\alpha_2$  subunit or for DDR1. In some lanes, as indicated, increased numbers of beads were analyzed to adjust for the reduced numbers of bound beads caused by MGO treatment. For the *top panel*, integrin  $\alpha_2$  subunit immunoblot, the preparations were as follows. Lane 1, PBS collagen beads, no adjustment; lane 2, 10 mM MGO collagen beads, no adjustment; lane 3, 1 mM MGO collagen beads, no adjustment; lane 4, 10 mM MGO collagen beads, 2-fold adjustment; lane 5, 1 mM MGO collagen beads, 2-fold adjustment; lane 6, 1 mM MGO collagen beads, 4-fold adjustment; lane 7, 10 mM MGO collagen beads, 4-fold adjustment; lane 8, BSA-coated beads; lane 9, 10 mM MGO-treated BSA-coated beads. For the *bottom panel*, DDR1 immunoblot, the preparations were as follows. Lane 1, PBS collagen beads, no adjustment; lane 2, 1 mM MGO collagen beads, no adjustment; lane 3, 10 mM MGO collagen beads, no adjustment; lane 4, PBS collagen beads, 2-fold adjustment; lane 5, 10 mM MGO collagen beads, 4-fold adjustment; lane 6, 1 mM MGO collagen beads, 4-fold adjustment; lane 7, 10 mM MGO collagen beads, 2-fold adjustment; lane 8, 1 mM MGO collagen beads, 2-fold adjustment; lane 9, 10 mM MGO collagen beads, 2-fold adjustment. Data are representative of three independent samples analyzed for integrin  $\alpha_2$  subunit and DDR1. *B*, collagen-coated beads were incubated with cells in the presence of irrelevant, isotype control antibody (*bar 1*) or in the presence of 1  $\mu\text{g}/\text{ml}$  4B4 antibody (*bar 2*; to block integrins containing  $\beta_1$  subunits) or with 10 mM MGO collagen beads (*bar 3*) or with 10 mM MGO collagen beads followed by 4B4 antibody (*bar 4*) or with collagen beads followed by 2  $\mu\text{g}/\text{ml}$  P1E6 antibody (*bar 5*; to block integrin  $\alpha_2$  subunit) or with 10 mM MGO collagen beads followed by P1E6 antibody (*bar 6*). Data are mean  $\pm$  S.E. of cells binding fluorescent beads. 4B4 and P1E6 antibody and MGO inhibited collagen bead binding ( $p < 0.001$  versus control collagen beads). Data were computed from three replicate cultures for each condition and are representative of three independent experiments. In each replicate, 10,000 cells were counted. *C*, immunostaining for ligand binding-induced epitope on integrin  $\beta_1$  subunit using the antibody 12G10 in human gingival fibroblasts. Cells were incubated with collagen-coated beads (CCB) (*top panel*) or MGO-treated beads (*lower panel*). Block arrows point to staining in the upper left panel and in bound beads for phase-contrast images (*right panels*). This experiment was repeated three times with similar results.

collagen coated beads to a chemical cross-linker (APG), which reacts with the guanidino group of Arg at pH 7–8. Cross-linking with APG (10 mM) inhibited collagen binding in human gingival fibroblasts by nearly 2-fold although not as effectively as MGO (PBS-treated collagen control =  $35.7 \pm 0.8\%$  of cell population; 1 mM MGO =  $12.5 \pm 0.4\%$  of cell population; 10 mM APG =  $20.8 \pm 1.2\%$  of cell population;  $p < 0.001$ ). We next determined the effect of MGO-induced cross-linking of Lys residues by treating collagen-coated beads with maleic anhydride, a reagent that protects Lys res-

idues from reacting with MGO. With beads pretreated with maleic anhydride and then treated with MGO overnight and finally incubated with cells, we found that very little of the MGO-induced inhibition of collagen binding was attributable to modifications of Lys residues (percentage of cells binding beads: control collagen =  $32.45 \pm 0.61\%$ ; 10 mM MGO-collagen =  $6.24 \pm 0.74\%$ ; maleic anhydride/MGO-treated collagen =  $6.77 \pm 0.73\%$ ). Further, reversal of the maleylation by incubating beads at pH 3 had an insignificant effect on the MGO effect on collagen binding.

# MGO Inhibits the Binding Step of Collagen Phagocytosis

**TABLE 4**

**MGO modification sites of collagen triple helical peptides**

The sequence was as follows: X-GPOGPOGPOGPOGARGERGFQGERGPOGPOGPOGPO (from C to N terminus, where O represents Hyp, X is CH<sub>3</sub>-(CH<sub>2</sub>)<sub>8</sub>-CO-, and Z is methylglyoxal).

Endoproteinase Glu-C digest <i>m/z</i> (measured)	<i>m/z</i> (calculated)	$\Delta m$	Peptide sequence	Modification sites
		<i>Da</i>		
678.324	678.321	0.003	18–23: (E)RGFOGE(R)	
732.337	732.332	0.005	18–23: (E)RGFOGE(R)	R <sup>18</sup> + Z-H <sub>2</sub> O
750.347	750.342	0.005	18–23: (E)RGFOGE(R)	R <sup>18</sup> + Z
804.358	804.353	0.005	18–23: (E)RGFOGE(R)	R <sup>18</sup> + 2Z-2H <sub>2</sub> O
822.365	822.363	0.002	18–23: (E)RGFOGE(R)	R <sup>18</sup> + 2Z
1242.627	1242.623	0.004	24–36: (E)RGPOGPOGPOGPO(<)	
1296.639	1296.634	0.005	24–36: (E)RGPOGPOGPOGPO(<)	R <sup>24</sup> + Z-H <sub>2</sub> O
1314.647	1314.644	0.003	24–36: (E)RGPOGPOGPOGPO(<)	R <sup>24</sup> + Z
1368.661	1368.655	0.006	24–36: (E)RGPOGPOGPOGPO(<)	R <sup>24</sup> + 2Z-H <sub>2</sub> O
1386.673	1386.665	0.008	24–36: (E)RGPOGPOGPOGPO(<)	R <sup>24</sup> + 2Z
1711.872	1711.866	0.006	1–17: X-GPOGPOGPOGPOGARGE(R)	X-
1765.890	1765.877	0.003	1–17: X-GPOGPOGPOGPOGARGE(R)	X-R <sup>15</sup> + Z-H <sub>2</sub> O
1783.898	1783.887	0.011	1–17: X-GPOGPOGPOGPOGARGE(R)	X-R <sup>15</sup> + Z
1837.909	1837.898	0.011	1–17: X-GPOGPOGPOGPOGARGE(R)	X-R <sup>15</sup> + 2Z-H <sub>2</sub> O
1855.917	1855.908	0.009	1–17: X-GPOGPOGPOGPOGARGE(R)	X-R <sup>15</sup> + 2Z

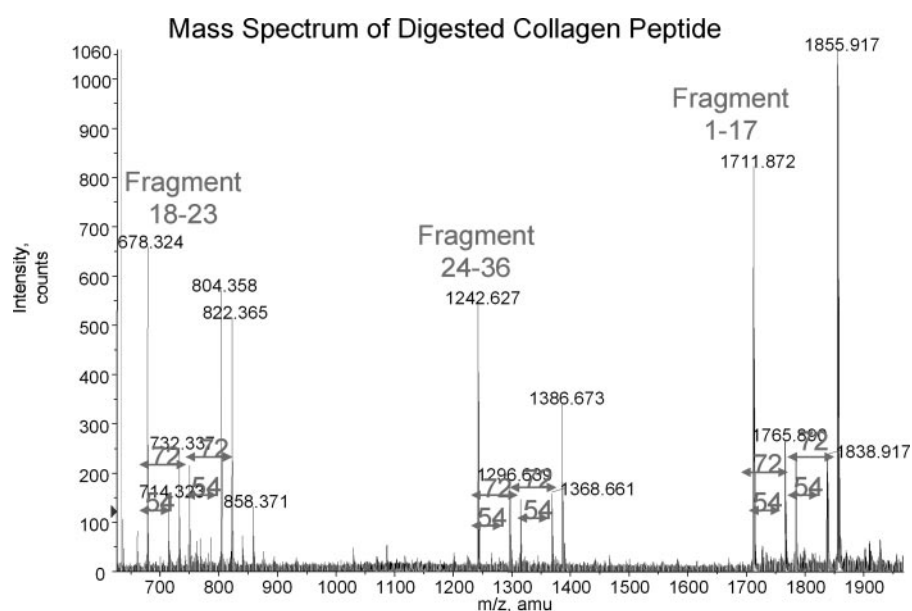


**FIGURE 6. Structural changes induced by MGO.** Triple helical peptides (36 amino acids) containing the Gly-Phe-Hyp-Gly-Glu-Arg sequence, the  $\alpha_2\beta_1$  integrin binding site of collagen, were treated with MGO (10 mM). Digestion with endoproteinase Glu-C and mass spectrometry analysis indicate that MGO treatment selectively modified arginine residues. No cross-linking of peptides was detected.

To focus on the effects of MGO on the  $\alpha_2\beta_1$  integrin binding site of fibrillar collagen, we used a triple helical collagen peptide that encompasses the  $\alpha_2\beta_1$  integrin binding site (Gly-Phe-Hyp-Gly-Glu-Arg) (Table 4) (40). We have shown previously the utility of this reagent for study of collagen phagocytosis by the  $\alpha_2\beta_1$  integrin (23). This peptide contains 3 Arg residues, one of which is located within the  $\alpha_2\beta_1$  integrin recognition sequence. Fluorescent beads coated with this peptide (1 mM incubation solution) bound only weakly to Rat 2 cells (~10% of cells bound collagen peptide beads), and MGO treatment reduced this to <1%. Mass spectrometry analysis of the MGO-treated peptide demonstrated that all Arg residues, including those within the integrin recognition sequence, were altered by binding with MGO (addition of one or two MGOs) and indicated the species derived from the loss of H<sub>2</sub>O from the modified peptides. This mass increment is consistent with the notion that these adducts

are probably Arg-derived hydroimidazolone residues of MG-H1 (41). However, it could not be ascertained whether there was preferential modification of a particular Arg residue within the peptide (Fig. 6, Table 3). Nevertheless, the modification of Arg residues was consistent with our finding that MGO treatment reduced the effectiveness of tryptic digestion of the MGO-treated peptide, as detected by mass spectrometry. Since the peptide contains no Lys residues, this finding underlines the importance of MGO-modified Arg residues in the inhibitory effects on collagen bead binding.

## DISCUSSION

The principal finding of this report is that MGO treatment of collagen inhibits the binding step of collagen phagocytosis, a critical process in maintaining connective tissue homeostasis (5, 19). Since the structure and remodeling of collagen-rich tissues, such as the periodontium, is strongly affected in periodontitis (1, 3, 5), we suggest that disruptions of collagen binding in phagocytic fibroblasts (5), possibly by bacterial and eukaryotic metabolites, such as MGO (2), may affect connective tissue homeostasis and contribute to pathology. Notably, MGO is an important metabolite of eukaryotic and bacterial cell metabolism (2) and is found in periodontal infections at increased concentrations (18). Since staining for MGO was only detectable in tissues directly adjacent to bacterially infected pockets, we suggest that a major contributor of MGO in periodontitis lesions is likely to be pathogenic bacteria. The concentrations of MGO used in the *in vitro* experiments reported here are much higher than those found physiologically, and it will be important to determine in the future if MGO

is indeed found at these concentrations in pathological situations (18), particularly since MGO at <1 mM can modify integrin binding sites (42).

We found that overnight incubations of collagen with 1 or 10 mM MGO decreased solubility and hydroxyproline content in pepsin-solubilized fractions of MGO-treated collagen, indicating enhanced cross-link formation. The MGO-induced formation of cross-links strongly affected the binding step of collagen phagocytosis and is consistent with previous findings showing that after only 10 h of MGO treatment, cell attachment to collagen is markedly reduced (30).

*Collagen Binding*—As described earlier (11, 12, 20), the  $\alpha_2\beta_1$  integrin is a critical receptor for mediating the binding step of collagen phagocytosis; this specificity was shown here using an integrin  $\alpha_2$  subunit-blocking antibody. The effect of MGO on collagen binding was apparently specific as measured in binding experiments using MGO-treated BSA beads, which showed no differences in binding compared with untreated BSA beads. Although we also considered that the discoidin domain receptor 1 (43) may be involved in the MGO inhibition of collagen binding, cells null for DDR1 showed no difference in the level of inhibition when compared with DDR1-expressing cells. Conceivably, other collagen receptors, including Endo 180 (44), may also be involved in mediating phagocytosis but were not examined here. Indeed, the role of Endo 180 as a gelatin receptor may explain the small proportion of integrin-independent binding that we found, possibly due to collagen denaturation in assays that were conducted near collagen's melting temperature.

Integrin interaction with ligands is dependent on both affinity and avidity, which, in turn, govern integrin function (45). Impaired adhesion strength and/or reduced receptor-ligand interactions may contribute to the decreased collagen binding observed with MGO-treated collagen. In measurements of binding strength with a shear force assay (4, 26), similar to BSA beads, MGO-treated collagen-coated beads were weakly bound and readily dislodged by shear forces. These data were consistent with studies of binding of multiple collagen-coated beads; in cells incubated with glycosylated collagen samples, there was no binding of multiple beads compared with control collagen. Since MGO causes collagen to become more insoluble, it is possible that MGO may enhance the association of collagen monomers within insoluble collagen structures, possibly by cross-linking. In this situation, available integrin binding sites on the surface of the beads would be reduced, because the surface to mass ratio of the collagen fiber is smaller than the monomer. This is a possible explanation for the reduction of collagen bead binding caused by MGO.

Cell spreading and lamellipodial extension around collagen fibrils is an important step in phagocytosis and subsequent intracellular digestion of collagen (19). We found that cells spread poorly on MGO-treated collagen, as reported earlier (30). Notably, the spreading processes that occur in early stages of collagen phagocytosis are regulated by intracellular calcium signaling (11, 36). Previous studies of endothelial cells have demonstrated an impairment of calcium signaling due to glycation of specific matrix proteins, but the mechanism that mediates this disruption is unknown (37, 46). We found that MGO-treated collagen blocked the increases of intracellular

calcium concentration seen in cells treated with control collagen beads, consistent with the notion that MGO inhibits collagen recognition and adhesion.

Since integrin activation is required for cell spreading (47, 48) and for the collagen binding step of phagocytosis (4, 25), we considered that antibody-induced activation of integrins could overcome potential MGO collagen-induced inactivation. However, the use of integrin-activating antibodies showed no enhancement of bead binding, indicating that independent of integrin activation status, MGO collagen is poorly recognized by collagen receptors.

*Mechanism of Binding Inhibition*—MGO-induced modifications of critical amino acids in collagen binding are the most likely cause of the binding inhibition. Treatment with aminoguanidine, a nucleophilic hydrazine compound that blocks the formation of glucose-derived collagen cross-links by derivatizing MGO (34), prevented MGO-induced inhibition of collagen binding. To identify the possible mechanisms involved in inhibition of collagen adhesion, we focused on the structural changes caused by MGO, primarily the cross-linking of Lys residues and modifications of Arg residues that are mediated by MGO (30). Cross-linking of collagen by APG, a chemical cross-linker that preferentially modifies Arg residues (49), also inhibited the binding step of collagen phagocytosis, supporting the notion that Arg modifications are important in MGO-induced impairment of collagen binding. The effect on Arg residues was investigated further in native collagen by protecting the Lys residues with maleic anhydride treatment (50) prior to MGO modification of Arg residues. The resulting Arg-specific alterations to collagen showed effects on collagen binding that were not statistically different from MGO-collagen in which both Lys and Arg residues were available for modification.

The sequence Gly-Phe-Hyp-Gly-Glu-Arg is the principal fibrillar collagen binding site for the  $\alpha_2\beta_1$  integrin (14–16) in fibrillar collagens I and II and is therefore critical for the binding step of collagen phagocytosis (12). We used a triple helical peptide (36 amino acids) that contains the  $\alpha_2\beta_1$  integrin binding site of type I collagen (40) and does not contain Lys residues. By mass spectrometry, we found that Arg residues in this sequence were modified by MGO, indicating that modification of Arg residues within the critical  $\alpha_2\beta_1$  integrin binding site of collagen may alter binding to cells. The modification to Arg residues by MGO with a mass difference of +54 has been previously reported (41). MGO modifications involved all three Arg residues in the peptide but with no apparent preference for a specific Arg residue. These MGO modifications of Arg residues in the binding sequence of collagen may have a direct effect on the binding capacity of the  $\alpha_2\beta_1$  integrin. Our data are consistent with recent data showing that MGO-induced modifications of the Arg-Gly-Asp sequence of type IV collagen inhibit integrin binding (51) and that MGO formed arginine-derived hydroimidazolone residues at modification sites in Arg-Gly-Asp and Gly-Phe-Hyp-Gly-Glu-Arg integrin-binding sites of collagen, causing endothelial cell detachment, anoikis, and inhibition of angiogenesis in endothelial cells (42).

Collectively, these findings demonstrate that MGO modification of Arg residues in the  $\alpha_2\beta_1$  integrin binding region of type I collagen molecules severely impairs collagen binding

that is required for phagocytosis of collagen fibers. Since phagocytosis is an important step for collagen degradation in mature tissues (5), the binding inhibition resulting from the modification of Arg residues could be responsible in part for the fibrosis that occurs in periodontitis.

*Acknowledgments*—We thank Greg Fields (Florida Atlantic University) for provision of the triple helical collagen peptides and Wolfgang Vogel (University of Toronto) for provision of the DDR1<sup>-/-</sup> and DDR1<sup>+/+</sup> cells. We are grateful to Laura Silver for assistance with preparation of the manuscript and the figures.

## REFERENCES

- Birkedal-Hansen, H., Moore, W. G., Bodden, M. K., Windsor, L. J., Birkedal-Hansen, B., DeCarlo, A., and Engler, J. A. (1993) *Crit. Rev. Oral Biol. Med.* **4**, 197–250
- Ferguson, G. P., and Booth, I. R. (1998) *J. Bacteriol.* **180**, 4314–4318
- Moskow, B. S., and Polson, A. M. (1991) *J. Clin. Periodontol.* **18**, 534–542
- Chou, D. H., Lee, W., and McCulloch, C. A. (1996) *J. Immunol.* **156**, 4354–4362
- Everts, V., van der Zee, E., Creemers, L., and Beertsen, W. (1996) *Histochem. J.* **28**, 229–245
- Gullberg, D., Gehlsen, K. R., Turner, D. C., Ahlen, K., Zijenah, L. S., Barnes, M. J., and Rubin, K. (1992) *EMBO J.* **11**, 3865–3873
- Kern, A., Eble, J., Golbik, R., and Kuhn, K. (1993) *Eur. J. Biochem.* **215**, 151–159
- Kapyla, J., Ivaska, J., Riikonen, R., Nykvist, P., Pentikainen, O., Johnson, M., and Heino, J. (2000) *J. Biol. Chem.* **275**, 3348–3354
- Nykvist, P., Tu, H., Ivaska, J., Kapyla, J., Pihlajaniemi, T., and Heino, J. (2000) *J. Biol. Chem.* **275**, 8255–8261
- Dickeson, S. K., Mathis, N. L., Rahman, M., Bergelson, J. M., and Santoro, S. A. (1999) *J. Biol. Chem.* **274**, 32182–32191
- Arora, P. D., Glogauer, M., Kapus, A., Kwiatkowski, D. J., and McCulloch, C. A. (2004) *Mol. Biol. Cell* **15**, 588–599
- Arora, P. D., Manolson, M. F., Downey, G. P., Sodek, J., and McCulloch, C. A. (2000) *J. Biol. Chem.* **275**, 35432–35441
- Shaw, S. K., Cepek, K. L., Murphy, E. A., Russell, G. J., Brenner, M. B., and Parker, C. M. (1994) *J. Biol. Chem.* **269**, 6016–6025
- Emsley, J., Knight, C. G., Farndale, R. W., Barnes, M. J., and Liddington, R. C. (2000) *Cell* **101**, 47–56
- Knight, C. G., Morton, L. F., Onley, D. J., Peachey, A. R., Messent, A. J., Smethurst, P. A., Tuckwell, D. S., Farndale, R. W., and Barnes, M. J. (1998) *J. Biol. Chem.* **273**, 33287–33294
- Knight, C. G., Morton, L. F., Peachey, A. R., Tuckwell, D. S., Farndale, R. W., and Barnes, M. J. (2000) *J. Biol. Chem.* **275**, 35–40
- Bailey, A. J., Paul, R. G., and Knott, L. (1998) *Mech. Ageing Dev.* **106**, 1–56
- Kashket, S., Maiden, M. F., Haffajee, A. D., and Kashket, E. R. (2003) *J. Clin. Periodontol.* **30**, 364–367
- Sodek, J., and Ferrier, J. M. (1988) *Collagen Relat. Res.* **8**, 11–21
- Lee, W., Sodek, J., and McCulloch, C. A. (1996) *J. Cell Physiol.* **168**, 695–704
- Pender, N., and McCulloch, C. A. (1991) *J. Cell Sci.* **100**, 187–193
- Knowles, G. C., McKeown, M., Sodek, J., and McCulloch, C. A. (1991) *J. Cell Sci.* **98**, 551–558
- Bhide, V. M., Laschinger, C. A., Arora, P. D., Lee, W., Hakkinen, L., Larjava, H., Sodek, J., and McCulloch, C. A. (2005) *J. Biol. Chem.* **280**, 23103–23113
- McKeown, M., Knowles, G., and McCulloch, C. A. (1990) *Cell Tissue Res.* **262**, 523–530
- Segal, G., Lee, W., Arora, P. D., McKee, M., Downey, G., and McCulloch, C. A. (2001) *J. Cell Sci.* **114**, 119–129
- Batista da Silva, A. P., Lee, W., Bajenova, E., McCulloch, C. A., and Ellen, R. P. (2004) *Cell Microbiol.* **6**, 485–498
- Phares, D. J., Smedley, G. T., and Flagan, R. C. (2000) *J. Fluid Mech.* **418**, 351–375
- Arora, P. D., Bibby, K. J., and McCulloch, C. A. (1994) *J. Cell Physiol.* **161**, 187–200
- Glogauer, M., Arora, P., Yao, G., Sokholov, I., Ferrier, J., and McCulloch, C. A. (1997) *J. Cell Sci.* **110**, 11–21
- Paul, R. G., and Bailey, A. J. (1999) *Int. J. Biochem. Cell Biol.* **31**, 653–660
- Monnier, V. M., and Cerami, A. (1981) *Science* **211**, 491–493
- Monnier, V. M., Kohn, R. R., and Cerami, A. (1984) *Proc. Natl. Acad. Sci. U. S. A.* **81**, 583–587
- Sell, D. R., and Monnier, V. M. (2004) *J. Biol. Chem.* **279**, 54173–54184
- Brownlee, M., Vlassara, H., Kooney, A., Ulrich, P., and Cerami, A. (1986) *Science* **232**, 1629–1632
- Ulrich, P., and Cerami, A. (2001) *Recent. Prog. Horm. Res.* **56**, 1–21
- Arora, P. D., Silvestri, L., Ganss, B., Sodek, J., and McCulloch, C. A. (2001) *J. Biol. Chem.* **276**, 14100–14109
- Bishara, N. B., Dunlop, M. E., Murphy, T. V., Darby, I. A., Sharmini Rajanayagam, M. A., and Hill, M. A. (2002) *J. Cell Physiol.* **193**, 80–92
- Vogel, W., Gish, G. D., Alves, F., and Pawson, T. (1997) *Mol. Cell* **1**, 13–23
- Mould, A. P., Garratt, A. N., Askari, J. A., Akiyama, S. K., and Humphries, M. J. (1995) *FEBS Lett.* **363**, 118–122
- Baronas-Lowell, D., Lauer-Fields, J., and Fields, G. (2004) *J. Biol. Chem.* **279**, 952–962
- Ahmed, N., Dobler, D., Dean, M., and Thornalley, P. J. (2005) *J. Biol. Chem.* **280**, 5724–5732
- Dobler, D., Ahmed, N., Song, L., Eboigbodin, K. E., and Thornalley, P. J. (2006) *Diabetes* **55**, 1961–1969
- Abdulhussein, R., McFadden, C., Fuentes-Prior, P., and Vogel, W. F. (2004) *J. Biol. Chem.* **279**, 31462–31470
- Engelholm, L. H., List, K., Netzel-Arnett, S., Cukierman, E., Mitola, D. J., Aaronson, H., Kjoller, L., Larsen, J. K., Yamada, K. M., Strickland, D. K., Holmbeck, K., Dano, K., Birkedal-Hansen, H., Behrendt, N., and Bugge, T. H. (2003) *J. Cell Biol.* **160**, 1009–1015
- Schwartz, M. A., Schaller, M. D., and Ginsberg, M. H. (1995) *Annu. Rev. Cell Dev. Biol.* **11**, 549–599
- Mene, P., Pascale, C., Teti, A., Bernardini, S., Cinotti, G. A., and Pugliese, F. (1999) *J. Am. Soc. Nephrol.* **10**, 1478–1486
- Arroyo, A. G., Sanchez-Mateos, P., Campanero, M. R., Martin-Padura, I., Dejana, E., and Sanchez-Madrid, F. (1992) *J. Cell Biol.* **117**, 659–670
- Uitto, V. J., and Larjava, H. (1991) *Crit. Rev. Oral Biol. Med.* **2**, 323–354
- Ngo, T., Yam, C., Lenhoff, H., and Ivy, J. (1981) *J. Biol. Chem.* **256**, 11313–11318
- Sodek, J., Hodges, R. S., and Smillie, L. B. (1978) *J. Biol. Chem.* **253**, 1129–1136
- Pedchenko, V. K., Chetyrkin, S. V., Chuang, P., Ham, A. J., Saleem, M. A., Mathieson, P. W., Hudson, B. G., and Voziyan, P. A. (2005) *Diabetes* **54**, 2952–2960